ISCI, Volume *19*

Supplemental Information

NCoR1: Putting the Brakes on the Dendritic Cell Immune Tolerance

Abdul Ahad, Mathias Stevanin, Shuchi Smita, Gyan Prakash Mishra, Dheerendra Gupta, Sebastian Waszak, Uday Aditya Sarkar, Soumen Basak, Bhawna Gupta, Hans Acha-Orbea, and Sunil Kumar Raghav

Figure S1: Related to Figure 1

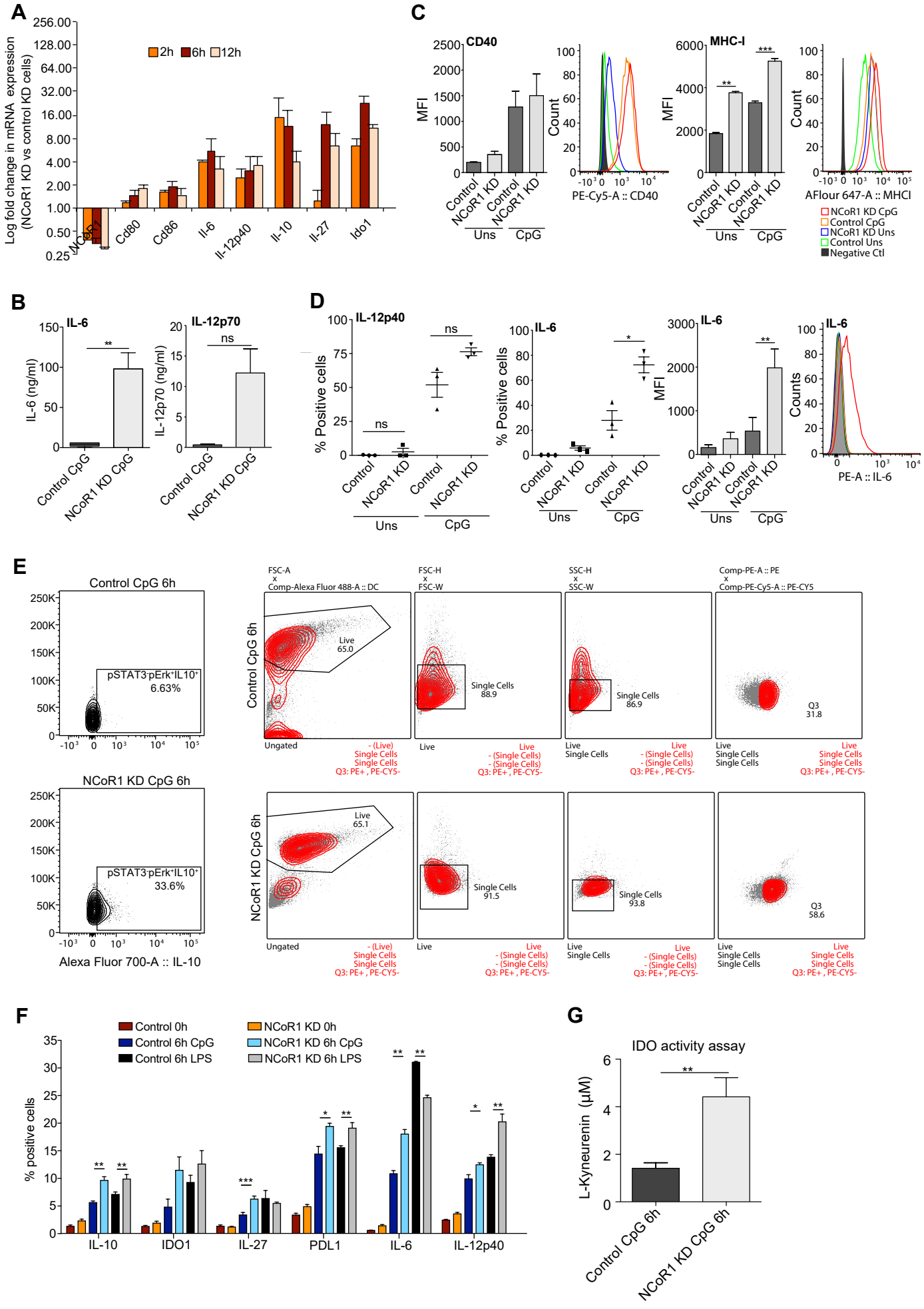

Figure S1. (Related to figure 1) NCoR1 KD cDCs (CD8α^+ and CD11b$^+$ DCs) show tolerogenic behavior after CpG activation *in vitro.*

A. RT-qPCR kinetics showing the transcript levels of selected DC response genes in NCoR1 KD and control cDC1 DC line after 2h, 6h and 12h CpG activation. (n=3)
B. Bio-Plex quantitation of secreted cytokines IL-6 and IL-12p70 in the culture supernatants of 6h CpG activated NCoR1 KD and control CD8α^+ DC. (n=6)
C. Bar plots showing the MFI shifts for co-stimulatory genes CD40 and MHC-I in in NCoR1 KD DCs and control cDC 1 DC line. (n=4) Corresponding histograms depict the representative MFI shifts.
D. Scatter-plots depicting the percentage positive cells for intracellular cytokines IL-6 and IL-12p40 in NCoR1 KD and control CD8α^+ cDC1 DCs before and after CpG stimulation. (n=4) Corresponding histograms depict the representative MFI shifts.
E. Contour-plots showing the percentages of pErk$^+$IL-10$^+$Stat3$^-$ cells in 6h CpG activated NCoR1 KD and control DCs. Gating strategy used to identify pErk$^+$STAT3$^-$IL-10$^+$ DCs in 6h CpG activated control and NCoR1 KD DCs. (n=3)
F. Bar-graph for flow cytometric data demonstrating percentage of positive cells for IL-10, IDO1, IL-27, PDL1, IL-6 and IL-12p40 in unstimulated, 6h CpG or LPS activated NCoR1 KD and control CD11b$^+$ cDC2 DCs. (n=3)
G. IDO activity assay showing the amount of L-Kynurenine produced in the culture supernatant of 6h CpG activated NCoR1 KD and control DCs. (n=3)

p-values are calculated using two tailed paired *t*-test. Error bars represent SEM.
*$\leq$ 0.05, **$\leq$ 0.01, ***$\leq$ 0.001

Figure S2. Related to Figure 1

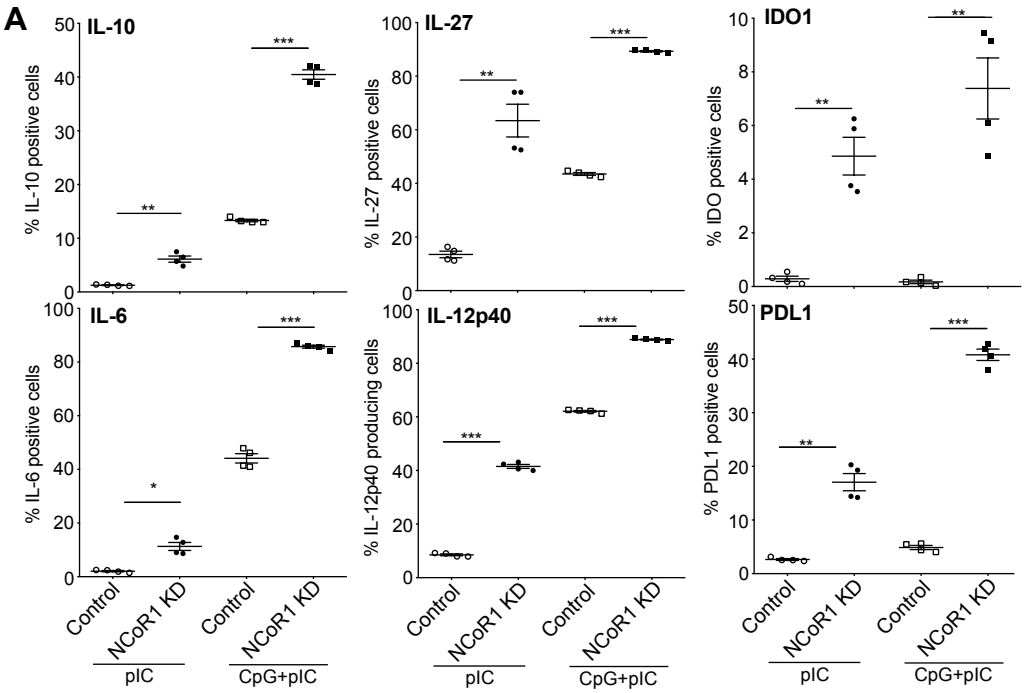

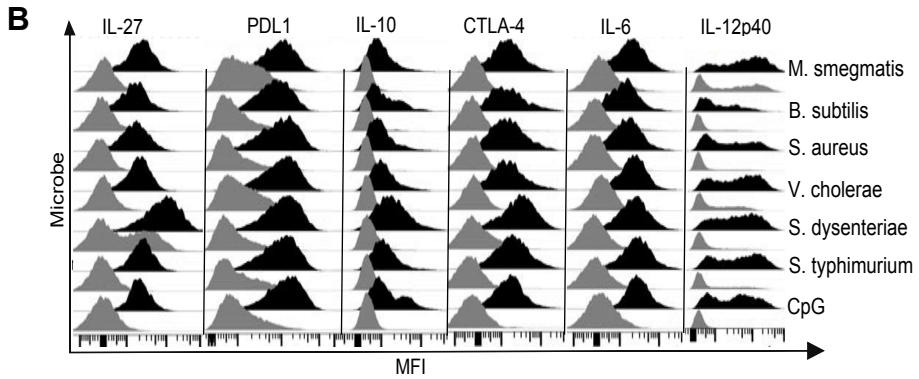

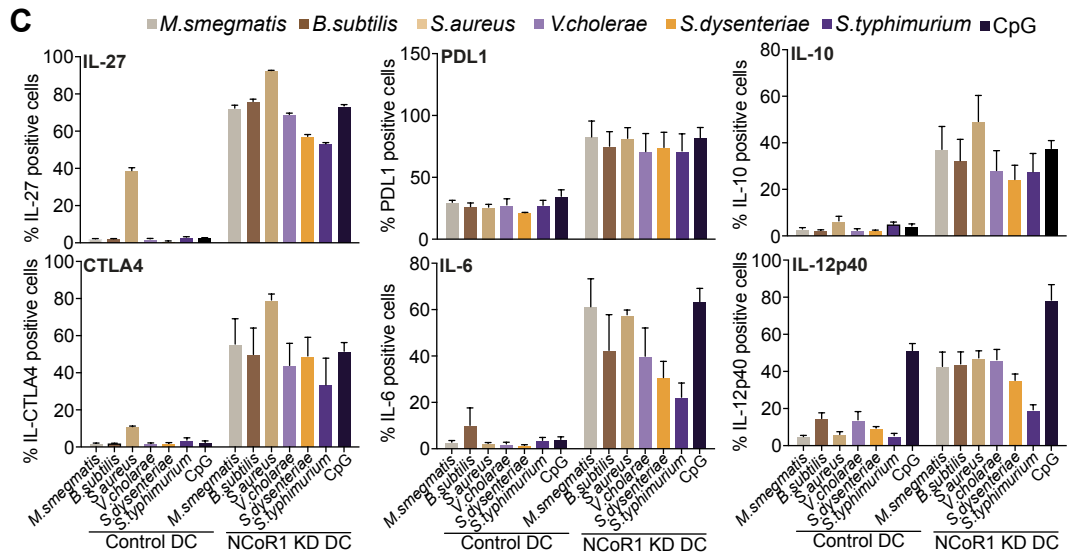

Figure S2. (Related to figure 1) NCoR1 KD cDC1 DCs develop strong tolerogenic behavior irrespective of activation by any strong TLR stimulus.

A. Scatter-plots prepared from flow cytometric analysis data showing the percentage positive cells demonstrating the expression of IL-10, IL-27, IDO1, IL-6, IL-12p40 and PDL1 in NCoR1 KD and control cDC1 DCs before and after 6h stimulation with pIC or CpG + pIC simultaneously.
B. Representative histogram plots depicting the MFI shifts for IL-27, PDL1, IL-10, CTLA4, IL-6 and IL-12p40 in NCoR1 KD and control cDC1 DC line before and after 6h challenge with heat killed gram-positive and gram-negative bacteria.
C. Bar graph depicting the percentage positive cells for IL-27, PDL1, IL-10, CTLA4, IL-6 and IL-12p40 in NCoR1 KD $CD8\alpha^{+}$ DC line as compared to control cells after 6h bacterial challenge. (n=3)

p-values are calculated using two tailed paired *t*-test. Error bars represent SEM.

*≤ 0.05, **≤ 0.01, ***≤ 0.001

Figure S3: Related to Figure 3

.

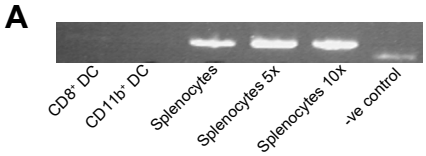

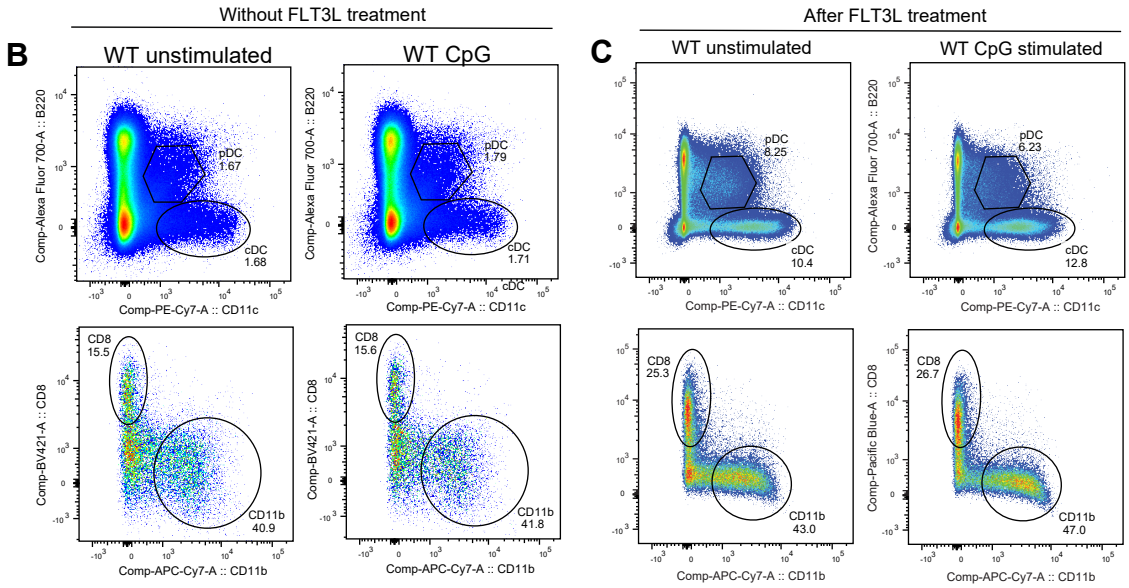

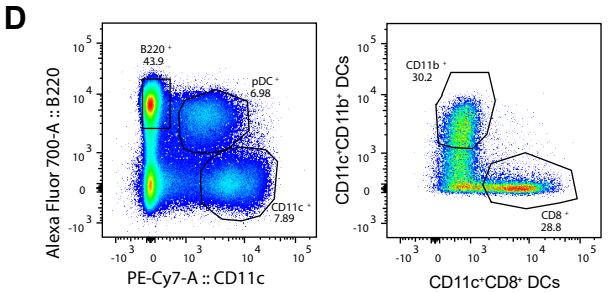

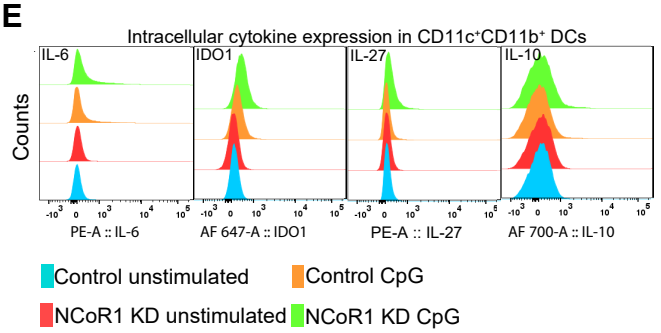

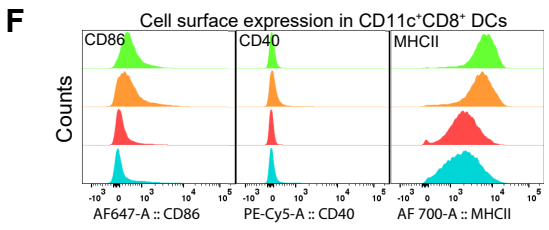

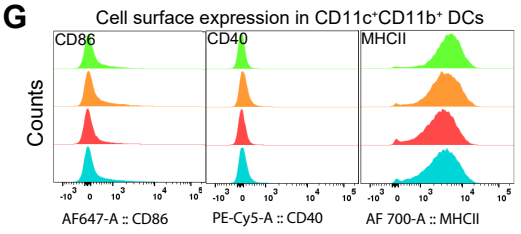

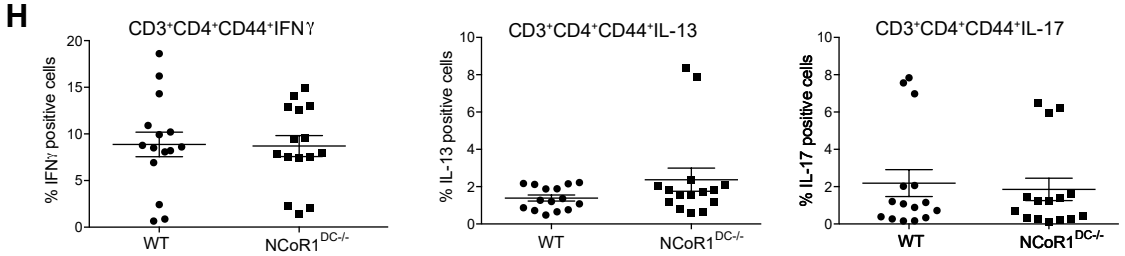

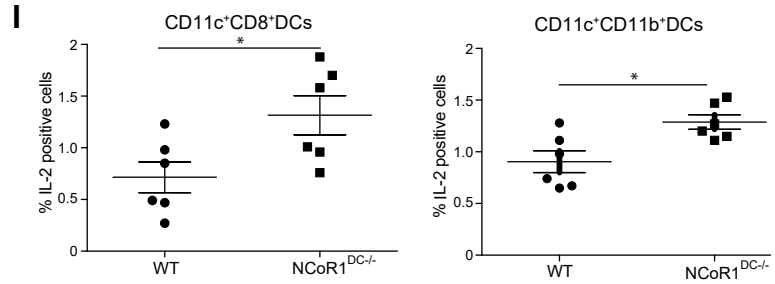

Figure S3 (Related to figure 3) CD11c^{+} DCs from NCoR1$^{DC-/-}$ mice show strong tolerogenic behavior upon CpG challenge.

A Agarose gel picture showing the presence or absence of the PCR products for the NCoR1 transcript in NCoR1$^{DC-/-}$ mice. The PCR was performed from DNA extracted from 4 x 10^5 CD8^{+} or CD11b^{+} FACS sorted DCs or splenocytes isolated from NCoR1$^{DC-/-}$ mice. Splenocytes 5X represents DNA from 2 x 10^6 Splenocytes 10X from 4 x 10^6 total splenocytes from NCoR1$^{DC-/-}$ mouse. No template control lane (-ve control) is PCR without template DNA.

B. & C.Representative dot-plots showing the percentage of pDCs, cDCs and further gated CD8^{+} and CD11b^{+} DCs in the cDC population before and after FLT3L treatment in WT and NCoR1$^{DC-/-}$ mice.

D. Dot-plots showing the gating strategy used for the flow cytometric analysis of different DC subsets from splenocytes of WT and NCoR1$^{DC-/-}$ mice.

E. Representative histograms showing the MFI differences in the intracellular expression of IL-6, IDO1, IL-27 and IL-10 in primary CD8^{+} cDCs gated in splenocytes treated with or without CpG for 6h from NCoR1$^{DC-/-}$ and WT mice. (n=6)

F. Flow cytometric analysis showing MFI shifts for cell surface markers CD40, CD86 and MHC-II in cDC1 DCs gated in splenocytes with or without 6h CpG stimulation from conditional NCoR1$^{DC-/-}$ and WT mice. (n=6)

G. Flow cytometric analysis showing MFI shifts for CD40, CD86 and MHC-II in primary cDC2 DCs gated in splenocytes with or without 6h CpG stimulation. (n=6)

H. FACS dot-plots depicting percentage of positive cells expressing IFNγ, IL-13 and IL-17 in effector T helper cell population from OVA + CpG vaccinated NCoR1$^{DC-/-}$ and WT mice. Five mice were used in each group each with three technical replicates. (n=5)

I. Flow cytometric analysis showing percent positive cells for IL-2 in cDC1 and cDC2 DCs gated in splenocytes isolated from conditional NCoR1$^{DC-/-}$ and WT mice and activated with or without CpG for 6h (n=6)

p-values are calculated using two sampled unpaired T-test. Error bars represent SEM.
*$\leq$ 0.05, **$\leq$ 0.01, ***$\leq$ 0.001

Figure S4: Related to Figure 3

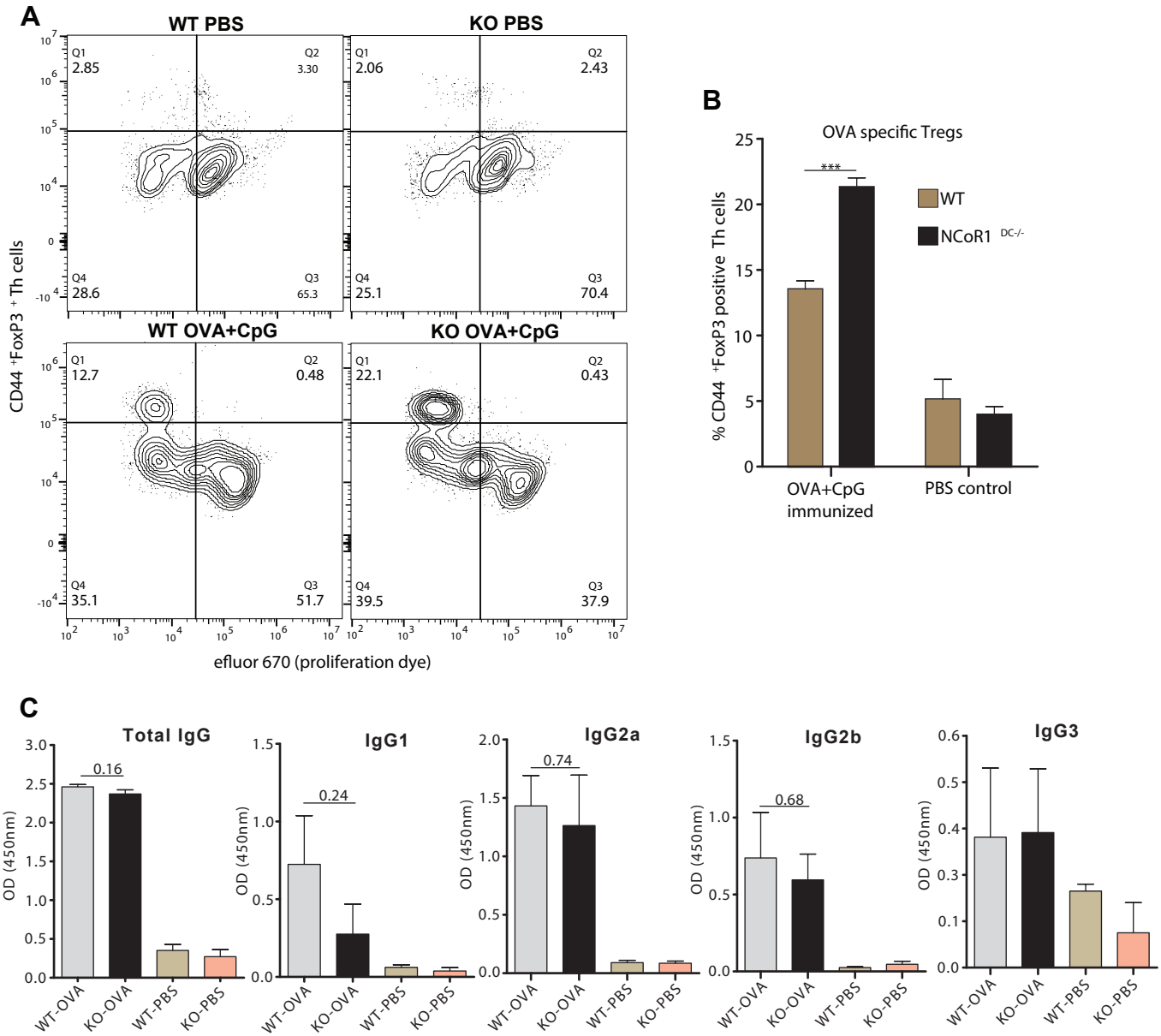

Figure S4. (Related to figure 3) T helper cell profiling of OVA+CpG immunized NCoR1$^{DC-/-}$ and WT animals.

A. FACS dot plots depicting the proliferation and percentage of FoxP3 positive population in effecter Th cells in isolated from lymph nodes of WT and NCoR1$^{DC-/-}$ OVA+CpG immunized animals. PBS immunized animals were used as controls. (n=5)

B. Bar graph showing the percentage positive FoxP3 cells in restimulated lymph node cells of WT and NCoR1$^{DC-/-}$ OVA+CpG immunized animals. PBS immunized animals were used as controls. (n=5)

C. ELISA results showing the OVA specific total IgG and isotype titres in serum of WT and NCoR1$^{DC-/-}$ OVA+CpG immunized animals. PBS immunized animals were used as controls. (n=5)

p-values are calculated using two sampled unpaired T-test. Error bars represent SEM.

*≤ 0.05, **≤ 0.01, ***≤ 0.001

Figure S5: Related to Figure 4.

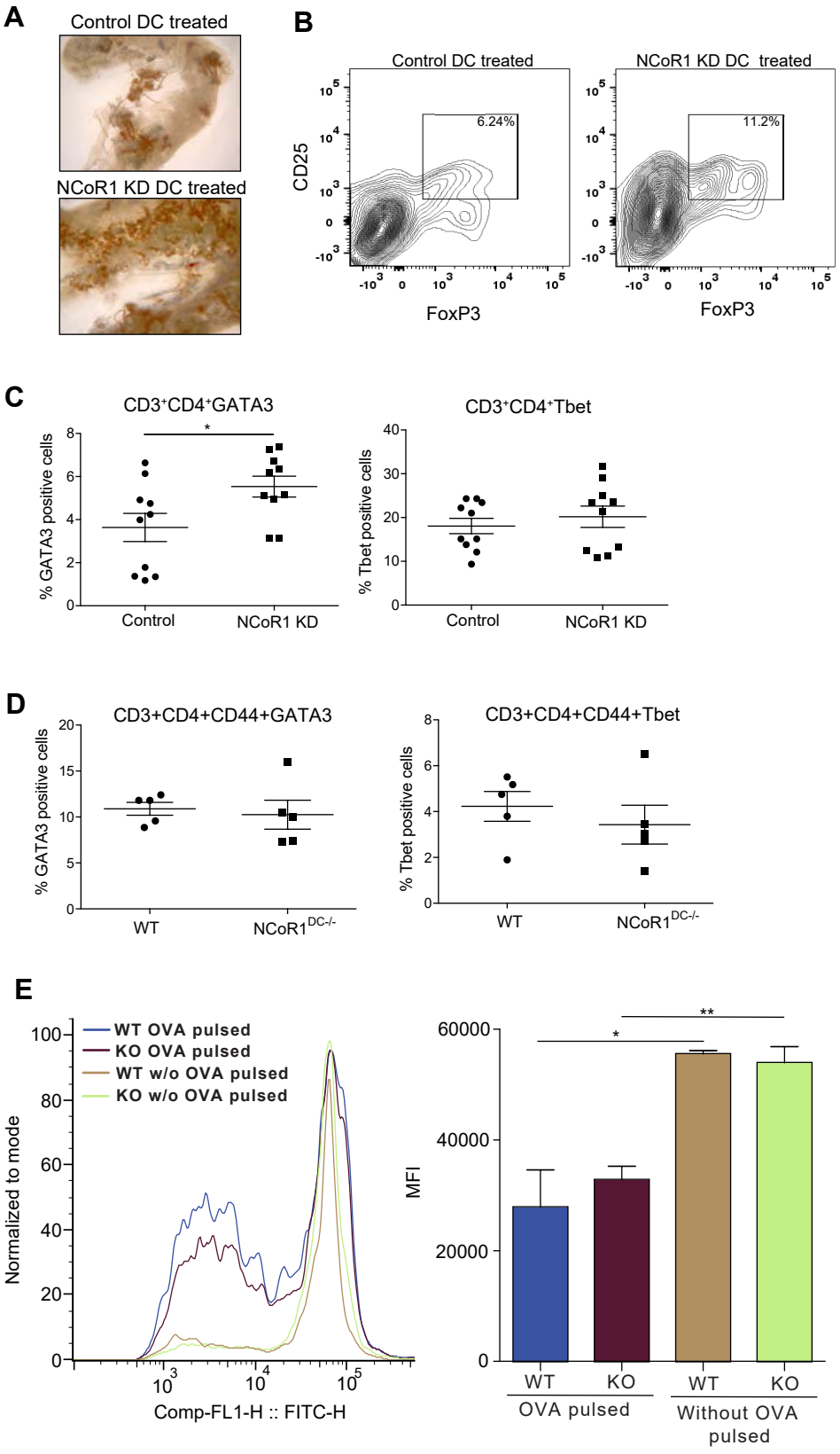

Figure S5. (Related to figure 4) NCoR1 KD/KO increases the egg and worm load by enhancing Treg population in Mesentric Lymph Nodes of helminth infected mice.

A. Representative pictures showing the helminth worms in the intestine of mice injected with CpG activated NCoR1 KD DCs as compared to control DCs. Images are representative of five mice from each group. The intestine was dissected and cut longitudinally to open it for worm counting and for taking the pictures. The images were taken from similar intestinal regions of different mice for comparison.

B. Contour-plot depicting the effector $CD25^{+}FoxP3^{+}$ Tregs in mesenteric lymph nodes (MLN) of CpG pulsed NCoR1 KD and control DC treated mice 15 days post helminth infection. (n=8)

C. Scatter-plots showing the percentage of positive T helper cells for GATA3 and Tbet from MLN of NCoR1 KD and control $CD8\alpha^{+}$ DC treated helminth infected mice after D15 (15 days) of infection. (n=10)

D. Scatter plots showing the percentage positive cells for GATA3 and Tbet producing CD4+CD44+ effector T cells from MLNs of helminth infected and CpG treated WT and $NCoR1^{DC-/-}$ mice D17 post infection. (n=5)

E. Histogram and bar plot showing the OT-II specific antigen presentation in helminth infected WT and $NCoR1^{DC-/-}$ mice (n=5)

p-values are calculated using two sampled unpaired *t*-test. Error bars represent SEM. *≤ 0.05, **≤ 0.01, ***≤ 0.001

Figure S6: Relative to Figure 6

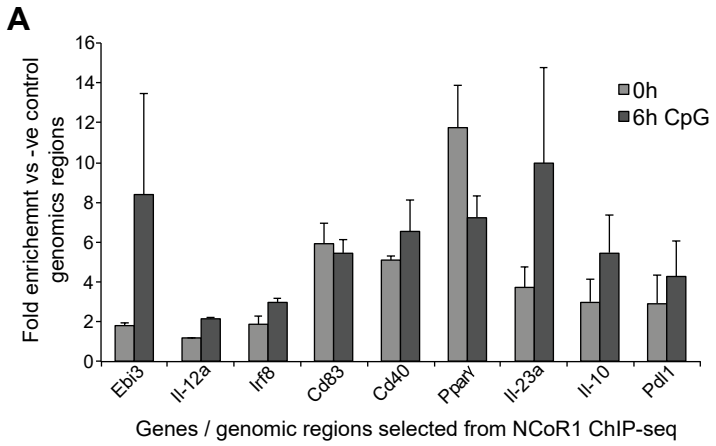

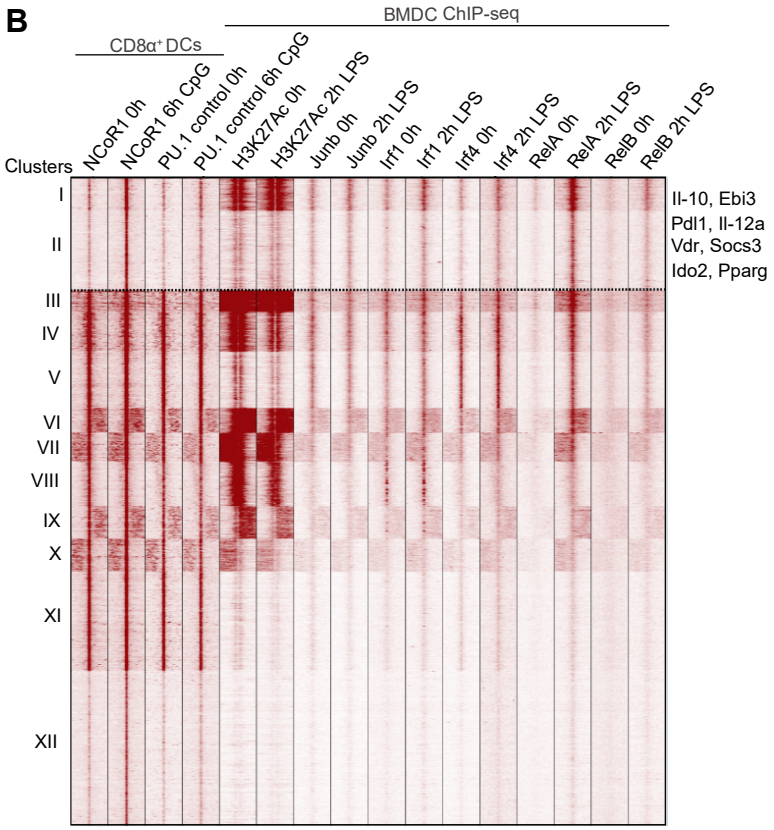

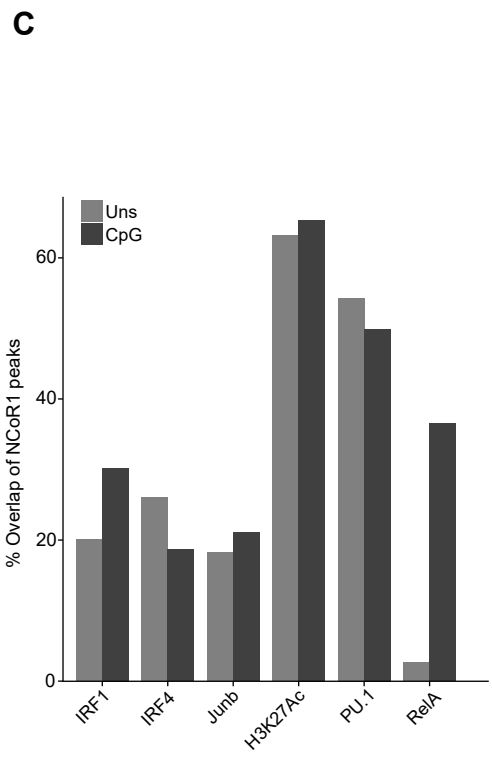

Figure S6. (Related to figure 6) PU.1 TF tethers NCoR1 to DNA in CD8α^+ DCs and NCoR1 directly represses tolerogenic genes after activation by masking the effects of activating TFs.

A. Bar plot showing the ChIP-qPCR fold change enrichment of NCoR1 at nine randomly selected genomic regions enriched in NCoR1 ChIP-seq data as compared to average of two negative control genomic regions. (n=2) Error bars shows standard deviation of NCoR1 enrichment in two independent biological replicates.
B. SeqMINER plot showing the global clustering of NCoR1, PU.1 binding at NCoR1 peaks in CpG activated CD8α^+ DCs. ChIP-seq data from unstimulated and 2h LPS stimulated primary BMDCs for H3K27ac histone mark and TFs PU.1, IRF1, IRF4, Junb, RelA and RelB was also clustered. Published and online available primary BMDC ChIP-seq data was reanalyzed using the pipeline used for the analysis of NCoR1 data.
C. Bar plot showing the percent overlap of NCoR1 with H3K27ac histone mark and TFs PU.1, IRF1, IRF4, Junb, RelA in 2h LPS stimulated primary BMDCs. Published and online available primary BMDC ChIP-seq data was reanalyzed using the pipeline used for the analysis of NCoR1 data.

Figure S7: Related to Figure 6.

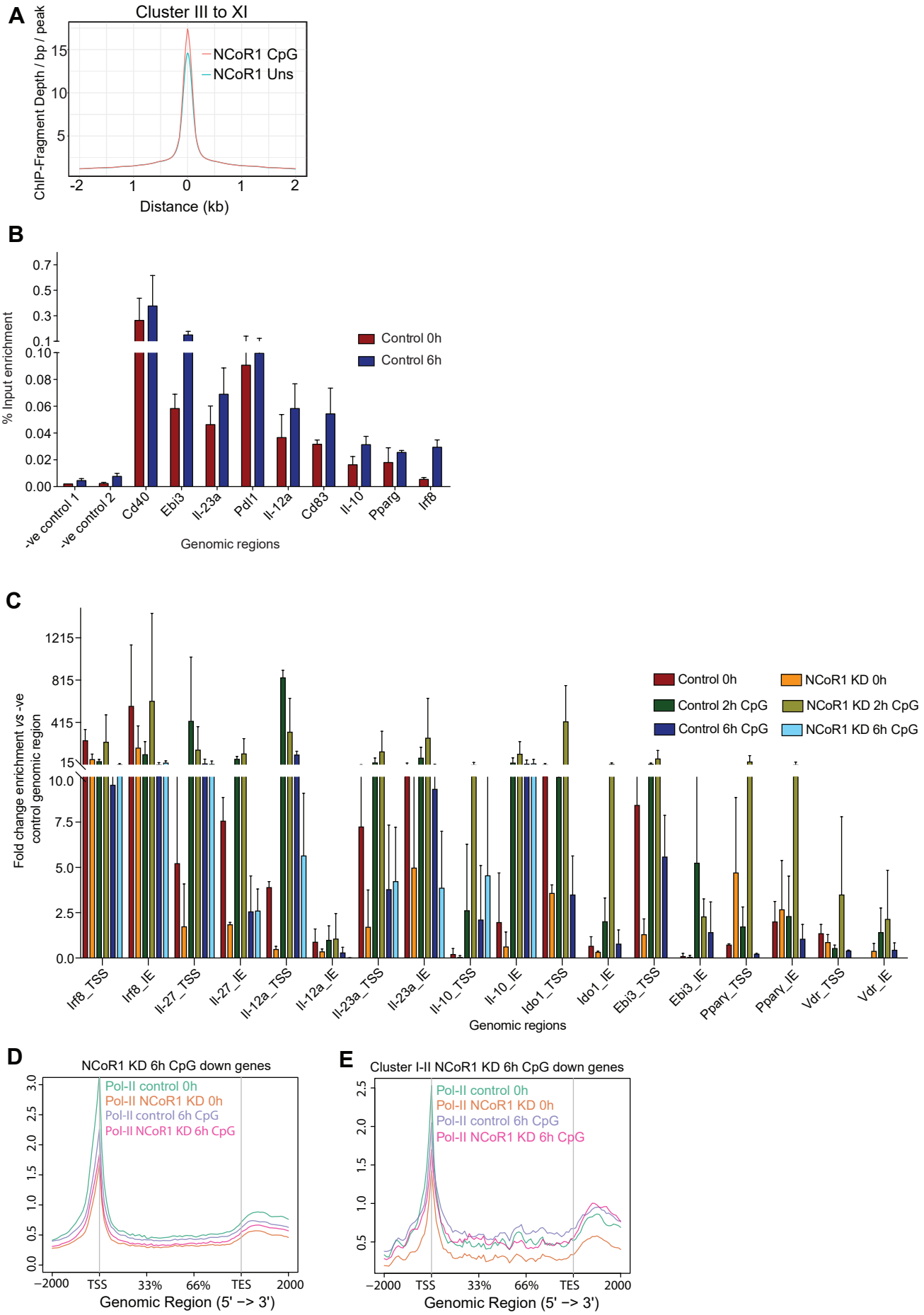

Figure S7. (Related to figure 6) NCoR1 represses PU.1 bound enhancers that are enriched for activating TFs such as RelA, IRFs, Jun after DC activation.

A. Density-plots showing the ChIP-seq intensity for NCoR1 peaks in seqminer clusters III to XI.
B. Bar plot showing the ChIP-qPCR fold change enrichment of PU.1 at nine randomly selected genomic regions enriched in NCoR1 ChIP-seq data as compared to average of two negative control genomic regions. (n=3) Error bars shows standard deviation of NCoR1 enrichment in three independent biological replicates.
C. ChIP-qPCR for RNA Pol-II in unstimulated and CpG activated (2h & 6h) control and NCoR1 KD DCs depicting the fold change enrichment of Pol-II at transcription start site (TSS) and gene body (intra-exonic, IE) of selected tolerogenic genes compared to negative control genomic region. (n=2)
D. Metagene plot depicting the RNA Pol-II profile in unstimulated and 6h CpG stimulated control and NCoR1 KD DCs for the total list of down-regulated genes in 6h CpG activated NCoR1 KD RNA-seq analysis.
E. Metagene plot showing the RNA Pol-II profile in unstimulated and 6h CpG stimulated control and NCoR1 KD DCs for the list of down-regulated genes in 6h CpG activated NCoR1 KD RNA-seq analysis and annotated to cluster I-II genomic regions

Supplementary table legends

Table S1. (Related to figure 5). The information of the CSV file containing the list of NCoR1 ChIP-seq peaks and the annotated genes in unstimulated (sheet 1) and 6h CpG activated (sheet 2) CD8α^+ DCs.

Table S2. (Related to figure 5). The information of the CSV file containing the list of differentially expressed genes significantly regulated in RNA-seq of 6h CpG challenged NCoR1 KD CD8α^+ DCs compared to control cells. Sheet-1: List of genes significantly upregulated (q-value $\leq$ 0.01 and $\geq$2 fold change) in NCoR1 KD compared to control DCs, Sheet-2: List of significantly down-regulated (q-value $\leq$ 0.01 and $\leq$2 fold change) genes in NCoR1 KD compared to control DC after CpG stimulation, Sheet-3: Genes significantly upregulated in RNA-seq list and are also bound by NCoR1 in ChIP-seq data of 6h CpG stimulated CD8α^+ DC, and Sheet-4: Genes significantly down-regulated in the RNA-seq list and are also bound by NCoR1 in ChIP-seq data of 6h CpG challenged CD8α^+ DC.

Table S3. (Related to figure 5). The information of the CSV file with the list of differentially expressed genes significantly regulated in RNA-seq analysis of unstimulated NCoR1 KD CD8α^+ DCs compared to control DCs. Sheet-1: List of genes significantly upregulated (q-value $\leq$ 0.01 and $\geq$ 2 fold change) in NCoR1 KD versus control DCs, Sheet-2: List of significantly down-regulated (q-value $\leq$ 0.01 and $\leq$2 fold) genes in NCoR1 KD compared to control KD DCs, Sheet-3: Genes bound by NCoR1 in ChIP-seq data and significantly upregulated in RNA-seq list, and Sheet-4: Genes bound by NCoR1 in ChIP-seq data and significantly down-regulated in RNA-seq list.

Table S4. (Related to figure 5). The information of the enriched pathways analysis through GeneGo Metacore analysis report CSV file with different sheets showing the list of biological pathway maps, process networks, diseases and GO processes significantly enriched for the 658 NCoR1 directly controlled and upregulated genes. ChIP-seq and RNA-seq correlation allowed identification of the genes directly controlled by NCoR1. Sheet-1: Biological pathway maps significantly enriched with their respective p-value and the genes involved, Sheet-2: Process networks significantly enriched with their respective p-value and the genes involved, Sheet-3: Diseases significantly enriched for the list of NCoR1 regulated genes with their respective p-value, and Sheet-4: GO Processes significantly enriched with their respective p-value.

Table S5. (Related to figure 5). The information of the enriched pathways analysis through GeneGo Metacore analysis report CSV file with different sheets showing the list of biological pathway maps, process networks, diseases and GO processes significantly enriched for the 439 NCoR1 unbound but upregulated genes. ChIP-seq and RNA-seq correlation lead us to identify the genes that are indirectly controlled by NCoR1. Sheet-1: Biological pathway maps significantly enriched with their respective p-values and the genes involved, Sheet-2: Process networks significantly enriched with their respective p-values and the genes involved, Sheet-3: Diseases significantly enriched for the list of NCoR1 regulated genes with their respective p-values, and Sheet-4: GO Processes significantly enriched with their respective p-values.

Table S6. (Related to figure 6). The information of the total list of genes in Excel file showing the that are annotated to cluster I-II shown in Fig. 6c and then differentially bound and regulated by NCoR1 in CpG condition and also enriched for other transcription factor PU.1 after activation. Sheet 1 shows total annotated genes whereas sheet 2 and sheet 3 shows genes that are bound and upregulated in NCoR1 KD and down-regulated after CpG activation respectively.

Table S7. (Related to figure 6). The information of the CSV file showing the list of genomic regions identified as super-enhancer (SE) or strongly repressed regions for NCoR1 and PU.1 respectively in unstimulated and CpG activated CD8α^+ DCs. We used the HOMER super enhancer discovery tool to identify the genomic regions and the genes that are showing strong enrichment (high rank for PU.1 and NCoR1). Sheet 1 and 2: Region list showing the NCoR1 strongly repressed (SR) regions and the annotated genes arranged according to their rank of repressor regions in unstimulated and CpG stimulated DCs respectively, Sheet 3 and 4: Region list showing the PU.1 super-enhancer (SE) regions and the annotated genes arranged according to their rank of enhancers in unstimulated and CpG stimulated DCs respectively.

Transparent Methods

Dendritic cell (DC) culture

The CD8α+ cDC1 and CD11b+ cDC2 DC lines were recently developed(Fuertes Marraco et al., 2012; Pigni et al., 2018).These cell lines perfectly mimic extraordinarily the immature cDC1 and cDC2 DCs isolated ex vivo from C57BL/6J mice(Fuertes Marraco et al., 2012; Pigni et al., 2018). The culture conditions were optimized for these immature DC lines. In brief, the cells were grown in IMDM medium supplemented with 10% FBS and antibiotic solution, 5 x 10-5 M β-mercaptoethanol, sodium bicarbonate, HEPES. The cells were maintained at 37°C in a humidified incubator with 5% CO2. These DCs were dissociated with a short incubation of 2-3 min in a non-enzymatic, 5 mM EDTA in 20 mM HEPES buffer. For in vitro experiments, the DCs were plated in 6-well plates at a density of 5 x 105 cells/ml overnight. The cells were then challenged with different activation media containing TLR9 agonist CpG-B, TLR3 agonist pIC, and CpG+pIC for different time points. For performing RT-qPCR analysis the cells were washed in the plate once with PBS followed by addition of RNA-later (RLT) buffer (Qiagen) for lysis of cells. The plates were then stored at -80oC until further RNA isolation and processing of samples.

Generation of stable NCoR1 KD CD8α+ and CD11b+ DCs

For generating stable NCoR1 knockdown (KD) and corresponding control DCs, lentiviral vector pLKO.1 (Sigma) containing NCoR1-specific shRNAs or control shRNA were used. Viral particles packaged with shRNA expressing transfer plasmids were produced in 293T cells using CalPhos mammalian transfection kit (Clontech) according to an optimized protocol (Barde et al., 2010) . 293T cells were transfected with transfer plasmids containing NCoR1 shRNAs or control shRNAs along with packaging plasmids (pCMVR8.74 and pMD2G). After 12-14h the culture medium was refreshed and the supernatant containing viral particles were collected after 24h in 50

ml conical tubes. The viral particle-containing culture supernatant was filtered through 0.45 µm syringe filters and preserved at -80°C in small aliquots. For transduction of shRNA containing viruses in CD8α+ or CD11b+ DC lines, the cells were plated at a density of 1.25 x 105 cells/well of 12 well plates followed by transduction with virus particles containing supernatant. The media was replaced with fresh media after 12h of virus incubation with DCs followed by addition of 1 µg/ml puromycin selection medium after 72h. The cells were puromycin selected for two to three weeks to get stable NCoR1 KD cells. The cells were also transduced with control shRNA-containing viruses to develop control cells for analysis comparisons. The efficiency of NCoR1 KD was quantified using NCoR1 gene specific primers by RT-qPCR. The shRNA that showed a significant and maximum decrease in NCoR1 gene transcript levels compared to control transduced cells were used for the further detailed study.

RNA isolation and RT-qPCR

Total RNA was isolated using RNeasy plus kit (Qiagen) according to vendor recommended protocol. The RNA concentration was estimated by nanodrop (Thermo) and then 1 µg of total RNA was used to prepare cDNA using SuperScript-III Reverse Transcriptase kit (Invitrogen). Quantitative PCR was performed using SYBR Green master mix (Roche) and PCR amplification was monitored in real-time using LightCycler-480 Instrument (Roche). Primer oligonucleotides for qPCR were designed using a universal probe library assay design system (Roche) and the primer pairs used are listed above in supplementary information. Primers were optimized for linear and single product amplification by performing standard curve assays.

Flow Cytometry (FACS)

Flow cytometric analyses of in vitro and ex vivo cultured cells were performed using routinely employed methods for FACS staining and analysis. After dissociation from

plates, the cultured cells were washed with FACS buffer (3% FCS in PBS, 5mM EDTA) followed by resuspension in surface staining buffer containing Fc receptor blocking antibody. After washing, fluorochrome conjugated antibodies for proteins of interest were added to the cells as a cocktail (see the list of antibodies for details). For intracellular (IC) staining of cytokines, the cells were first fixed with 2% paraformaldehyde followed by permeabilization using 1x permeabilization buffer (eBiosciences). The fixed cells were then resuspended in intracellular staining buffer containing Fc receptor blocking antibody and stained with fluorochrome tagged antibodies for selected cytokines. For optimal staining, the cells were incubated with antibodies for 30 min in dark at room temperature. After incubation, the cells were washed three times with FACS wash buffer and then acquired for differential expression analysis on LSRII flow cytometer (BD Biosciences). The acquired data were analyzed using FlowJo-X software (Treestar). All antibodies used in flow cytometry experiments are listed in resource table.

Bio-Plex (Luminex) assay for cytokine quantitation from cell culture supernatants

Bio-Plex assay (multiplex ELISA) was used to estimate the cytokines levels secreted in the cell culture supernatants of NCoR1 KD and control DCs before and after CpG stimulation. After culture the supernatants were stored at -80□C in small aliquots until analysis. Cytokine levels were estimated using 23-plex-mouse cytokine assay kit following the vendor recommended protocol (Biorad).

Indoleamine 2,3-dioxygenase (IDO) activity assay

IDO activity in cell culture supernatants of NCoR1 KD and control cells before and after 6h CpG stimulation was performed using the protocol described before(Feng and Taylor, 1989) . Fifty □l culture supernatants from NCoR1 KD and control CD8α+ DCs

were mixed with 30 ml of 30% trichloroacetic acid in 96 well plates followed by spin at 4000 rpm for 8 min. After centrifugation half of the supernatant was mixed with equal volume of Ehrlich reagent (0.8% p-dimethyl aminobenzaldehyde in acetic acid) for 30 min to allow conversion of L-tryptophan to L- kynurenine. The optical density (OD) of developed colored product was measured using spectrophotometer at 490 nm. Standard curve using known concentration of L- kynurenine was prepared to calculate the L- kynurenine using the observed ODs. Samples and standards were treated at the same time.

Generation of DC specific NCoR1 knockout mice (NCoR1$^{DC-/-}$)

DC specific conditional knockout (KO) C57BL/6J mice for NCoR1 gene (NCoR1$^{DC-/-}$) were generated using Cre-Lox recombination system(Birnberg et al., 2008) . Animals having Cre-recombinase driven under the minimal DC-specific CD11c promoter were used to delete the NCoR1 gene specifically in DCs(Yamamoto et al., 2011) . NCoR1fl/fl mice were crossed with CD11c-Cre mice and resulting heterozygous progenies were back-crossed for several generations to obtain pure homozygous NCoR1$^{DC-/-}$ mice. Genotyping PCRs were performed for NCoR1 and Cre gene using DNA isolated from sorted CD11c+ DCs and total splenocytes to identify the deletion status of NCoR1 gene in animals (Supplementary Fig. 3a). For getting sufficient number of DCs ex vivo from NCoR1$^{DC-/-}$ mice were treated with FLT3L serum (equivalent to 50 mg/ml FLT3L) for 10 days. Spleens were then harvested and digested with collagenase-D for 20 min at 37°C. After obtaining a single cell suspension, conventional DCs were FACS sorted using cell surface markers i.e., B220-CD11c+CD8+ and B220-CD11c+CD11b+ cells. Then DNA was extracted from 4 x 105 FACS sorted DCs for genotyping PCR. DNA was extracted using the DNeasy Blood & Tissue DNA isolation kit (Qiagen) according to the recommended protocol. After NCoR1 gene PCR, samples were loaded on a 2% agarose gel to visualize the presence or absence of PCR product. After confirmation

of the NCoR1 ablation by the absence of PCR product the experiments were performed on 6-15 weeks old sex-matched mice. For all the in vivo and ex vivo mice experiments we strictly followed the guidelines approved by the Swiss Federal and Cantonal veterinary or the ILS guidelines authorities.

For ex-vivo DC experiments using wild type (WT) and NCoR1DC-/- mice, the animals were treated with FLT3L alternatively for 8 days as described before for getting sufficient number of DCs. Single cell suspensions were made from spleen and lymph nodes of NCoR1DC-/- mice. Spleens were incubated with collagenase-D solution for 20 min at 37□C followed by mild mincing with the syringe plunger. The suspension was then treated with 1x RBC lysis buffer (Tonbo). Lymph nodes were minced into small pieces with sterile scalpel or scissors in a culture dish. Cell clumps were then passed through 70 μm strainer to obtain single cell suspensions.

Co-culture of DCs with CD4+ T cells for assessing T cell proliferation and differentiation

DC-T cell co-culture experiments were performed as described before(Smita et al., 2018). Naïve CD4+ T cells were purified from spleen of TCR-transgenic OTII mice using CD4+ T cell isolation kit (Miltenyi Biotec). NCoR1 KD and control CD8α+ DCs were seeded at a density of 20,000 cells/well in round bottom 96 well plates followed by incubation with OVA (aa 323-339) peptide with and without CpG for 2h. After 2h, purified OT-II T cells were added at the density of 100,000 cells/well (1:10 ratio). For T cell proliferation, CD4+ T cells were labeled with eFluor-670 proliferation dye (eBiosciences, Cat no: 65-0840-85) before co-culture with DCs. Proliferation rate and T helper cell differentiation into different subtypes were analyzed by FACS after 5 days. Fluorochrome conjugated antibodies specific to different T cell subtypes were used to profile T cells into Th1 (Tbet and IFNγ), Th2 (GATA3, IL-13), Tregs (CD25, FoxP3) and Th17 (IL-17). For gating effector T cell gating we used CD44 marker antibody (see

reagent list for details of antibodies).

CpG and OVA immunization to ascertain the in vivo impact of NCoR1 gene ablation on T cell differentiation

To identify the functional impact of NCoR1 ablation on T helper cell differentiation, we performed CpG + OVA vaccination. Different vaccine formulations were tested for ovalbumin (OVA), however, the most replicable method remained a simple mixture of 50 µg CpG and 10 µg OVA in PBS. NCoR1DC-/- and WT mice were vaccinated subcutaneously at the base of the tail at day 0 followed by a booster dose at day 30. Three mice from each group were used in each experiment and experiment was repeated five times. Three days after the booster injection, inguinal lymph nodes were harvested and T cell differentiation pattern into Th1, Th2 or Tregs was analyzed by flow cytometry.

OVA specific T cell response and ELISA

To examine OVA specific immune response we performed experiments as described (Alignani et al., 2005) (Maletto et al., 2002) (Semmrich et al., 2012) . In brief, we collected sera at D33 after OVA immunization from NCoR1DC-/- and WT animals to perform ELISA for OVA specific IgG titer. Elisa plates were coated with 100ug/ml of OVA (Sigma) prepared in bicarbonate / carbonate coating buffer for overnight at 4°C following five washes with washing buffer (PBS with 0.05% tween -20). Blocking was done with PBST containing 0.5% gelatin for 1h at 37°C. After five times washing, 1:10 diluted sera were added from NCoR1DC-/- and WT mice and kept for 1.5 h at 37 °C. Total IgG was detected using anti-mouse HRP conjugated IgG whereas IgG isotypes were detected using biotin labelled anti-mouse IgG1, IgG2a, and IgG2b following with anti-mouse streptavidin-HRP (Biolegend). The plates were read using ELISA reader for IgG estimation.

For OVA specific T cell proliferation and FoxP3 levels, we performed the experiment as described before (Huang et al., 2010) . In brief, cells were harvested from inguinal lymph nodes of NCoR1DC-/- and WT mice at D33 and stained with proliferation dye ef-670 (ebioscience). These stained cells were co-cultured with OVA pulsed DCs for three days. After three days, CD4 T cells were stained and analyzed for proliferation and FoxP3 levels.

Specificity for antigen presentation by DCs from WT and NCoR1DC-/- mice were examined by injecting 5 X 106 purified CD45.1+ CFSE labelled OT-II T cells in helminth infected CD45.2+ WT and NCoR1DC-/- mice at D12 of infection through tail vein. Next day 1 X 106 wild type DCs pulsed with OVA peptide or media alone were transferred through same route. After five days i.e. day 17, we took splenocytes from WT and KO mice and checked for peptide specific proliferation of FACS gated CD45.1+ cells.

Chromatin Immuno-Precipitation (ChIP) for NCoR1, PU.1, RNA Pol-II, and RelA

The ChIP for NCoR1 and TFs was performed according to the method optimized previously by Raghav and colleagues (Raghav and Deplancke, 2012). Several NCoR1 antibodies were optimized for performing NCoR1 pull-down for efficient ChIP assays and therefore in this study, we have used the same antibody(Raghav and Deplancke, 2012). For ChIP assays, 30 x 106 CD8α+ cDC1 DCs were seeded in 15 cm2 plates and prepared for ChIP before and after 2h & 6h after CpG or pIC stimulation. PU.1 and RNA Pol-II ChIPs were also performed in NCoR1 depleted and matched control DCs at similar time points. For ChIP, the cells were cross-linked using 1% formaldehyde (Sigma) for 10 min at room temperature followed by quenching the reaction using 2.5 M glycine (Sigma) for 10 min. The plates were placed on ice and the cells were scraped and collected in 50 ml conical tubes. The cells were then washed three times using cold 1 x PBS and cell pellets were stored at -80°C. At the day of ChIP experiment, the

cells were thawed on ice followed by lysis in nuclei extraction buffer (50 mM HEPES-NaOH pH 7.5, 140 mM NaCl, 1 mM EDTA pH 8.0, 10% glycerol, 0.5% NP-40, 0.25% TritonX-100) supplemented with protease and phosphatase inhibitors (Roche) for 10 min at 4°C on rocker shaker. The prepared nuclei were then washed using protein extraction buffer (200 mM NaCl, 1 mM EDTA pH 8.0, 0.5 mM EGTA pH 8.0, 10 mM Tris-HCl pH 8.0) supplemented with a protease and phosphatase inhibitors (Roche) at room temperature for 10 min. Washed nuclei were resuspended in chromatin extraction buffer (1 mM EDTA pH 8.0, 0.5 mM EGTA pH 8.0, 10 mM Tris-HCl pH 8.0 and 1% TritonX-100) supplemented with protease and phosphatase inhibitors (Roche) and incubated for 20 min on ice for equilibration. The chromatin was fragmented using a Bioruptor (Diagenode) sonicator for 30 min using high amplitude and 30s ON & 30s OFF cycles to obtain 200-500 bp size fragments. A cooling unit was used to circulate the cold water during sonication to avoid de-crosslinking because of overheating. After sonication, chromatin length was checked in agarose gel. The fragmented chromatin was centrifuged at 10,000 rpm for 5 min and then clear supernatant was collected in 15 ml conical tubes. The DNA concentration of the chromatin was estimated using a NanoDrop (Thermo) and the chromatin was diluted with ChIP dilution buffer (1 mM EDTA pH 8.0, 10 mM Tris-HCl pH 8.0 and 1% TritonX-100 containing protease and phosphatase inhibitors) to use 150 µg/ml of chromatin for each IP. BSA and ssDNA (Salmon Sperm DNA) pre-blocked protein-A sepharose (80 µl/IP) beads were added to the samples on ice and incubated for 2h to remove non-specific-binding chromatin. To the supernatant, 5 µl of rabbit polyclonal anti-NCoR1 (Abcam, cat no: ab-24552), 25 µl of anti-PU.1 (Santa Cruz, sc-390659), or RNA Pol-II (Cell signaling, 2629S) were added to immuno-precipitate the chromatin complex at 4°C overnight on rocker shaker. After the overnight incubation, 50 µl blocked protein-A sepharose beads were added to each sample and incubated for 2.5h at 4°C to pull down the respective antibody-chromatin complexes. The beads were then washed three times with low salt wash buffer (20 mM Tris-Cl pH 8.0, 150 mM NaCl, 2 mM EDTA pH 8.0, 0.1% SDS, 1%

TritonX-100) followed by two washes with high salt wash buffer (20 mM Tris-Cl pH 8.0, 500 mM NaCl, 2 mM EDTA pH 8.0, 0.1% SDS, 1% TritonX- 100), lithium chloride wash buffer (10 mM Tris-Cl pH 8.0, 0.25 M LiCl, 1 mM EDTA pH 8.0, 1% NP-40, 1% sodium deoxycholate) and Tris-EDTA (TE) buffer (10 mM Tris-Cl pH 8.0, 1 mM EDTA pH 8.0). After removing the wash buffer completely, protein-bound chromatin complexes were eluted from beads for 30 min using elution buffer (100 mM sodium bicarbonate and 1% SDS in milliQ water). The eluted chromatin was the reverse-crosslinked by incubating the eluted supernatant at 65°C overnight on a heat block after adding 8 µl of 5 M NaCl. Next day DNA was purified from the reverse cross-linked chromatin by proteinase-K and RNase digestion followed by purification using PCR purification kit (Qiagen). The purified DNA was eluted in 40 µl of elution buffer.

ChIP-/RNA-seq library preparation for Next Generation Sequencing (NGS)

For RNA-seq library preparation 2 µg of total RNA was used to isolate mRNA through magnetic beads using mRNA isolation kit (PolyA mRNA isolation Module, NEB) followed by RNA-seq library preparation using mRNA library preparation kit (NEB) strictly following the vendor recommended protocol. After library preparation concentration of libraries was estimated using qubit 2.0 (Invitrogen) and the recommended fragmentation sizes were confirmed by Bio-analyzer (Agilent). For ChIP-seq library preparation, 30 µl ChIP-DNA was processed for library preparation according to ChIP-seq library preparation recommended protocol (NEB). After library preparation and quality check, the libraries were sent to NGS service provider (Genotypic technology, Bangalore, India) for Illumina sequencing using NextSeq-500 instrument.

ChIP-qPCR validations

For experimental validation of PU.1 and RNA Pol-II ChIP-seq results, ChIP-qPCR was

performed at 0h and 6h after CpG activation of control and NCoR1 KD DCs. Enrichment of these factors at randomly selected ChIP-seq positive genomic regions/genes was calculated in comparison to negative control genomic regions. Three independent ChIP experiments were performed for PU.1 ChIP-qPCR whereas two independent biological replicates were used for RNA Pol-II validation. For RNA Pol-II ChIP-seq libraries were prepared from ChIP-DNA samples followed by qPCR for selected genomic regions annotated to TSS and intra-exonic regions of selected DC response/tolerogenic genes using 0.5ng DNA per reaction from each sample. Fold enrichment at positive genomic regions was calculated relative to negative control regions. Similarly for PU.1 1:10 diluted purified ChIP-DNA was used to perform qPCR for the selected DC response/tolerogenic genes and negative control genomic regions (-ve ctrl1 & 2). For RNA Pol-II ChIP-qPCR, the p-value significance was calculated by comparing the enrichment of positive genomic regions in NCoR1 KD as compared to control cells. Whereas in case of PU.1 as we did not observe any overall enrichment differences in ChIP-seq, therefore, the p-value significance was calculated by comparing the enrichment of positive control genomic regions compared to negative control regions in three biological replicates. The ChIP primers used are listed in reagent list in the resource table. The p-value for enrichment significance was calculated using two-tailed paired Students t-test and error bars depicted SEM in the fold change error in enrichments observed in different biological replicates.

Similarly to validate the NCoR1 ChIP-seq results, we performed ChIP-qPCR using two independent biological replicates and checked the enrichment of ten randomly selected positive control regions as compared to two negative control genomic regions. We found that all the ten positive genomic regions were >2 fold enriched compared to an average of negative control regions (Supplementary Fig. 6e). These analyses confirmed the robustness of our NCoR1 ChIP-seq data.

Electrophoretic Mobility Shift Assay (EMSA)

Previously described method and NFkB site containing probe were used for EMSA (Banoth et al., 2015) . In brief, Cells were treated with first cytoplasmic extraction buffer (10mM HEPES-KOH pH 7.9, 60mM KCL, 1mM EDTA. 0.5%NP-40, 1mM DTT supplemented with protease inhibitor) with three rounds of vortex and incubation on ice. Cytoplasmic fraction was collected and the pellet was washed once with CE buffer and then resuspended in Nuclear extraction buffer (250mM Tris-cl pH7.5, 60mM KCL, 1mM EDTA, 1mM DTT supplemented with protease inhibitor) which further subjected to three cycles of freeze-thaw. For DNA binding assay of NFkB subunits, nuclear extracts were pre-incubated with P32-labeled double-stranded NFkB oligonucleotide probe in binding buffer [20mM Tris-Cl (pH 7.5), 100mM NaCl, 20% glycerol, 2% NP-40, 1mM EDTA, 0.1mg/ml Poly dI:dC (Santa Cruz)] and NFkB subunit was marked depending on the position of shifted bands. For determining the level of NFkB in the nucleus, nuclear extract was resolved in SDS-PAGE and immunoblotted with NFkB subunit specific antibodies.

DC microbial infection assay

Total six bacterial strains were used to ascertain the immune response changes in NCoR1 KD and control DCs with live bacterial challenge for 6h. We used three gram-positive (M. smegmatis, B. subtilis, S. aureus) and three gram-negative (V. cholera, S. dysinteriae, S. typhi) bacteria. A multiplicity of infection (MOI) 3 was used to infect DCs. CpG stimulation was used as a control for comparison. After 2h of infection, the culture medium was removed and cells were washed with media followed by addition of fresh medium. Cells were then kept for 4h at 37°C in a humidified incubator with 5% CO2. For FACS analysis the cells were treated with Brefeldin-A for 4h to prevent the secretion of cytokines in the supernatant. After 6h of bacterial activation RT-qPCR and flow cytometric analysis was performed as described above. For RT-qPCR analysis, Brefeldin-A was not added to the cells.

Heligmosomoides polygyrus helminth infection in NCoR1DC-/- and WT mice

For helminth infection, NCoR1DC-/- and WT female mice were infected with 200 infective L3 larvae of H. polygyrus in PBS per mice through oral gavage. At day 10 after infection mice were treated with 50 μg CpG-1826. The feces from treated animals were collected daily for counting worm eggs in McMaster chambers. After observing a significant difference in egg count between NCoR1DC-/- and WT animals, mice were sacrificed for detailed T cell profiling of MLNs. The intestinal helminth worms were counted from the intestine of five animals from each group. The T cell differentiation into Th1, Th2, Tregs and Th17 subtypes were assessed using FACS as detailed above.

Leishmania major infection model in NCoR1DC-/- and wt mice

L. major was provided by the group Tacchini-Cottier (WHO, University of Lausanne). For infection in NCoR1DC-/- and wt mice, 3 x 106 parasites were injected in the right footpad of each mouse. Thickness difference between the right and the left footpad was measured every 4-5 days. At day 18 mice were administered 50 μg CpG intraperitoneally. At the end of the experiments, footpads and popliteal lymph nodes were harvested to measure the parasite load. Parasite loads were quantified by qPCR and T-cell differentiation profiling was performed on popliteal lymph nodes by flow cytometry (see the details above for flow cytometric analysis method).

Adoptive transfer of DCs in helminth infection mice model

For DC Adoptive transfer experiments we took 6-8 weeks old female mice and infected them with 200 infective L3 larvae/mice in PBS through oral gavage. At day 7 after infection mice were treated with 100 □g of anti-CD8b antibody/mice followed by adoptive transfer of 10 x 106 CpG pulsed NCoR1 KD and control CD8α+ DCs in sterile

PBS intraperitoneally. Two booster doses of 5 x 10^6 cells pulsed with CpG were adoptively transferred again intraperitoneally each after 48h. After adoptive transfer of DCs, the feces were collected and eggs were counted after every 24h time period using a well-optimized protocol. After observing a significant difference in egg count between NCoR1 KD treated and control animals, five mice from each group were sacrificed for detailed T cell profiling from mesenteric lymph nodes and the helminth worms were counted from the intestine of the dissected animals. The intestines were longitudinally opened and flipped to count the worms and to take pictures. The T cell differentiation into Th1, Th2, Tregs and Th17 subtypes was assessed using FACS as detailed above. This mouse experiment was performed following the animal ethical guidelines after taking due approval from the institutional animal ethics committee at ILS, Bhubaneswar, India.

Pre-processing of ChIP-seq data

Sequenced ChIP tags from NCoR1 (Input, Unstimulated, and CpG activated DCs at 6h), PU1, and RNA pol-II in control and NCoR1 KD (0h and 6h CpG stimulation) were aligned to reference mouse genome (mm10) using Bowtie2(Langmead and Salzberg, 2012) with default parameter (bowtie2 --qc-filter -t -q -x). Duplicates reads were filtered out and uniquely aligned reads were extracted using Samtools. To carry out further downstream analysis, low quality reads and duplicates were removed and uniquely aligned reads were taken in both unstimulated and CpG stimulated samples. To compare sample, NCoR1 ChIP-seq reads were down-sampled to 35 million reads using Picard tool. ChIP-seq datasets from primary bone marrow-derived DCs (BMDCs) for transcription factors PU.1, IRF1, IRF4, JunB, RelA, and active enhancer histone mark H3K27ac before and after 2h LPS stimulation(Garber et al., 2012) were downloaded from Gene Expression Omnibus (GEO6104). Reads from all the samples sequenced in different lanes were merged together then aligned to mouse (mm10)

genome as performed for NCoR1 data.

ChIP-seq peak calling and annotation

Peak calling was performed using HOMER suite (Heinz et al., 2010) . In case of NCoR1 ChIP-seq samples, peaks were called using -factor option and fold enrichment over input ChIP tag count of 4 and FDR of 0.01 was used to get significantly enriched peaks. Total peaks obtained in were filtered based on regions falling in blacklisted regions and regions with DNA copy number variation. In case of PU1, Pol-II, and primary BMDC ChIPseq data, peaks were called using –factor option for transcription factor and –histone for H3K27ac ChIP-seq. The peaks were called in these samples based on fold enrichment of 4 over surrounding 10kb region (as given in HOMER peak finding protocol).

Total enriched peaks in NCoR1 and primary BMDC ChIPseq data were annotated to nearest gene using HOMER's annotate Peaks.pl(Heinz et al., 2010) with the default option. Peak regions were divided into promoter proximal peaks based on genes annotating between -1000 to 300 (distance to TSS) and promoter distal peaks annotating to genes other than -1000 to 300.

For PU.1 ChIP-seq validations, we performed independent ChIP-seq biological replicates using wild type and empty vector transduced control DCs at 0h and 6h after CpG activation to overlap and confirm that the PU.1 binding detection is robust and consistent in control and empty vector transduced DCs in our experiments. We found a Spearman correlation of $\geq$0.8 between PU.1 ChIP-seq peaks identified by HOMER (data not shown).

Pol-II ChIP-seq data analysis

RNA pol-II ChIPseq data in control and NCoR1 KD condition (0h, 2h, and 6h of CpG stimulation) were processed in the same manner as mentioned earlier.

De novo motif analysis

We performed de novo and known motif prediction using “findMotifsGenome.pl” of Homer suite(Heinz et al., 2010) (size -100 –len 8, 10, 12). Top known motifs from JASPAR having P-value lessthan 1e-20 as well as shared at majority of peak region (% target peaks) were taken as an enriched motif at NCoR1 peaks.

RNA-Seq analysis

Raw RNA-seq reads were aligned to RefSeq gene annotation of the NCBI38/mm10 GTF file downloaded from UCSC genome browser using tophat 2.1 (Kim et al., 2013) with default parameter (tophat -o tophat_out -G mm10_refseq mm10 R1_1.fastq.gz R1_2.fastq.gz). To carry out differential gene expression study we used Cufflink 2.2.1 suite(Trapnell et al., 2010). Assembly of each transcript and expression level estimation was carried out using cufflinks. Transcripts from both the samples were merged using Cuffmerge and differential gene expressions were carried out using Cuffdiff. To retrieve significant differentially expressed gene, the raw file generated from the Cuffdiff output were filtered using q value cutoff of 0.05 and log2 (fold change) cutoff of 1 and -1 for up-regulated genes and down-regulated genes respectively.

Pathway enrichment analysis for differentially regulated genes

To identify the pathway maps, networks, GO and disease enriched for the genes that are directly regulated (upregulated or downregulated) by NCoR1 in CpG activated CD8α+ DCs, we used GeneGo Metacore analysis software program. The gene lists were uploaded in the tool and then enrichment analysis was performed as per the manual of the software. The reports were generated as CSV file and presented here as supplementary tables 5 and 6.

Overlap of NCoR1 and PU.1 ChIP-seq from CD8α+ DCs and comparison

with ChIP-seq peaks of H3K27ac and TF marks in BMDCs

To validate enrichment of PU.1 at NCoR1 bound regions in ChIP-seq, we overlapped the peak regions of PU.1 in control and NCoR1 KD DCs before and after 6h CpG activation. We also overlapped H3K27Ac, PU.1, IRF1, IRF4 and RelA ChIP-seq data from 0h and 2h LPS stimulated primary BMDCs. We calculated the percentage of NCoR1 peaks overlapping with these transcription factors (Supplementary Fig. 6c) using R package ChIP-seeker. Further, we then visualized the tag density of these factors at NCoR1 peaks using SeqMINER 1.3.3 (Supplementary Fig. 7b, c)(Ye et al., 2011). Online available raw ChIP-seq data from primary BMDCs were analyzed using a method similar to our NCoR1 ChIP-seq data to remove any bias due to analysis. BAM files generated were then used to overlap the enriched genomic regions. K-means clustering was done to cluster the genomic regions according to the similarity in enrichment. NCoR1 binding peaks in CpG was used as a reference and the genomic regions 2kb on both left and right side of NCoR1 peaks was probed for any overlap. We restricted our analysis to 12 clusters and clusters were then arranged according to their similarity. As per difference of binding pattern in clusters I and II, we annotated these regions to genes using "annotatePeaks.pl" of HOMER. The nearest annotated genes were compared to differentially expressed gene list from our RNAseq data.

Identification of super-enhancer regulatory elements bound by NCoR1 and PU.1

Total peaks in unstimulated and CpG activation condition were stitched and super-enhancer regions were identified using ROSE (Whyte et al., 2013). We ran ROSE with a stitching distance of 12.5kb and we excluded the peaks in the region of ±2000bp around the transcription start site. Super-enhancer regions were ranked based on tag density (lowest to highest).

Annotation of identified super-enhancer regions

The identified regulatory elements that are strongly repressed (SR) by NCoR1 and super-enhancer regions bound by PU.1 were annotated to nearest genes using annotatePeaks.pl of HOMER suite. NCoR1 and PU.1 signal at enhancer regions versus regions ranked by respective signal were plotted and tolerogenic genes falling in super-enhancer regions were highlighted.

Statistical analysis

The data in different figures with biological replicates are presented as the mean ± SEM. Statistical significance of the data was analyzed using two-tailed paired Student's t-test in case of cell line data whereas for animal experiments unpaired student's t-test was used to calculate significance. Data with significantly unequal variance was transformed prior to statistical analysis. For PU.1 ChIP-qPCR we calculated the p-value significance by comparing the enrichment of positive genomic regions with negative control regions, as we did not find any major change in binding before and after NCoR1 KD. In the case of RNA Pol-II ChIP-qPCR enrichment at positive genomic regions in NCoR1 KD were compared to control cells to calculate the significance. p-values are depicted in figures as * $\leq$ 0.05, ** $\leq$ 0.01 and *** $\leq$ 0.001

Data and code availability

The sequencing data (Raw data and processed files) used in this publication is submitted to the NCBI Gene Expression Omnibus (GEO; http://www.ncbi.nlm.nih.gov/geo/). The accession number for the sequence reported in this publication is GSE110423 and the authors declare that all the data supporting the findings of this study will be accessible to the readers within the article or its Supplementary information files and from the corresponding author on reasonable request.

Supplemental References:

Alignani, D., Maletto, B., Liscovsky, M., Ropolo, A., Moron, G., and Pistoresi-Palencia, M.C. (2005). Orally administered OVA/CpG-ODN induces specific mucosal and systemic immune response in young and aged mice. J Leukoc Biol 77, 898-905.

Banoth, B., Chatterjee, B., Vijayaragavan, B., Prasad, M.V., Roy, P., and Basak, S. (2015). Stimulus-selective crosstalk via the NF-kappaB signaling system reinforces innate immune response to alleviate gut infection. Elife 4.

Barde, I., Salmon, P., and Trono, D. (2010). Production and titration of lentiviral vectors. Curr Protoc Neurosci Chapter 4, Unit 4 21.

Birnberg, T., Bar-On, L., Sapoznikov, A., Caton, M.L., Cervantes-Barragan, L., Makia, D., Krauthgamer, R., Brenner, O., Ludewig, B., Brockschnieder, D., et al. (2008). Lack of conventional dendritic cells is compatible with normal development and T cell homeostasis, but causes myeloid proliferative syndrome. Immunity 29, 986-997.

Feng, G.S., and Taylor, M.W. (1989). Interferon gamma-resistant mutants are defective in the induction of indoleamine 2,3-dioxygenase. Proc Natl Acad Sci U S A 86, 7144-7148.

Fuertes Marraco, S.A., Grosjean, F., Duval, A., Rosa, M., Lavanchy, C., Ashok, D., Haller, S., Otten, L.A., Steiner, Q.G., Descombes, P., et al. (2012). Novel murine dendritic cell lines: a powerful auxiliary tool for dendritic cell research. Front Immunol 3, 331.

Heinz, S., Benner, C., Spann, N., Bertolino, E., Lin, Y.C., Laslo, P., Cheng, J.X., Murre, C., Singh, H., and Glass, C.K. (2010). Simple combinations of lineage-determining transcription factors prime cis-regulatory elements required for macrophage and B cell identities. Mol Cell 38, 576-589.

Huang, H., Ostroff, G.R., Lee, C.K., Specht, C.A., and Levitz, S.M. (2010). Robust stimulation of humoral and cellular immune responses following vaccination with antigen-loaded beta-glucan particles. MBio 1.

Kim, D., Pertea, G., Trapnell, C., Pimentel, H., Kelley, R., and Salzberg, S.L. (2013). TopHat2: accurate alignment of transcriptomes in the presence of insertions, deletions and gene fusions. Genome Biol 14, R36.

Langmead, B., and Salzberg, S.L. (2012). Fast gapped-read alignment with Bowtie 2. Nat Methods 9, 357-359.

Maletto, B., Ropolo, A., Moron, V., and Pistoresi-Palencia, M.C. (2002). CpG-DNA stimulates cellular and humoral immunity and promotes Th1 differentiation in aged BALB/c mice. J Leukoc Biol 72, 447-454.

Pigni, M., Ashok, D., Stevanin, M., and Acha-Orbea, H. (2018). Establishment and

Characterization of a Functionally Competent Type 2 Conventional Dendritic Cell Line. Front Immunol 9, 1912.

Raghav, S.K., and Deplancke, B. (2012). Genome-wide profiling of DNA-binding proteins using barcode-based multiplex Solexa sequencing. Methods Mol Biol 786, 247-262.

Semmrich, M., Plantinga, M., Svensson-Frej, M., Uronen-Hansson, H., Gustafsson, T., Mowat, A.M., Yrlid, U., Lambrecht, B.N., and Agace, W.W. (2012). Directed antigen targeting in vivo identifies a role for CD103+ dendritic cells in both tolerogenic and immunogenic T-cell responses. Mucosal Immunol 5, 150-160.

Trapnell, C., Williams, B.A., Pertea, G., Mortazavi, A., Kwan, G., van Baren, M.J., Salzberg, S.L., Wold, B.J., and Pachter, L. (2010). Transcript assembly and quantification by RNA-Seq reveals unannotated transcripts and isoform switching during cell differentiation. Nat Biotechnol 28, 511-515.

Whyte, W.A., Orlando, D.A., Hnisz, D., Abraham, B.J., Lin, C.Y., Kagey, M.H., Rahl, P.B., Lee, T.I., and Young, R.A. (2013). Master transcription factors and mediator establish super-enhancers at key cell identity genes. Cell 153, 307-319.

Yamamoto, H., Williams, E.G., Mouchiroud, L., Canto, C., Fan, W., Downes, M., Heligon, C., Barish, G.D., Desvergne, B., Evans, R.M., et al. (2011). NCoR1 is a conserved physiological modulator of muscle mass and oxidative function. Cell 147, 827-839.

REAGENT & RESOURCES	SOURCE	IDENTIFIER
Antibodies		
Anti-CD3 FITC (clone:17A2)	e-Bioscience	11-0032-82
Anti-Foxp3 PE (clone:150D/E4)	e-Bioscience	12-4774-42
Anti-mouse IL13 PE-Cyanine7 (clone:ebio13a)	e-Bioscience	25-7133-82
Anti-mouse IL13 eFluor 450	e-Bioscience	48-7133
Anti-mouse IL27p28 PE (clone:MM27-7B1)	e-Bioscience	12-7285-80
Anti-mouse IL6 PE (clone:MP5-20F3)	e-Bioscience	12-7061-81
Anti-mouse CD80 PE (clone:16-10A1)	e-Bioscience	12-0801-82
Anti-mouse CD40 PerCP-eFluor710 (clone:1C10)	e-Bioscience	46-0401-82
Anti-mouse CD274(B7-H1)/PDL1 PerCP-eFluor710 (clone:MIH5)	e-Bioscience	46-5982-82
Anti-Hu/Mo Gata-3 PE-eFlour610 (clone: TWAJ)	e-Bioscience	61-9966-41
Anti-mouse MHCII (I-A/I-E) AlexaFluor700 (clone:M5/114.15.2)	e-Bioscience	56-5321-82
Anti-Hu/Mo CD44 eFluor450 (clone:IM7)	e-Bioscience	48-0441-82
Anti-Mo/Hu CD44 PE-Cy7	e-Bioscience	25-4031-82
Anti-mouse IL10 AlexaFluor 700 (clone:JES5-16E3)	e-Bioscience	56-7101-80
Anti-mouse MHCI(H-2Kb) APC (clone: AF6-88.5.5.3)	e-Bioscience	17-5958-80
TCRb-BV510	Biolegend	109234
Anti-mouse CD3 PE (clone:17A2)	e-Bioscience	50-0032-U025
Anti-Hu/Mo Tbet PE-Cyanine7 (clone:eBio4b10)	e-Bioscience	25-5825-82
Anti-mouse CD25 APC (clone:GL-1(GL1))	e-Bioscience	20-0862-0100
Anti-mouse CD4 PE-Cyanine7 (clone:GK1.5)	e-Bioscience	25-0041-82
Anti-mouse IFN gamma APC (clone:XMG1.2)	e-Bioscience	17-7311-81
Anti-mouse IFN gamma PE	e-Bioscience	12-7311-82
Anti-mouse CD11c APC (clone:N418)	e-Bioscience	17-0114-82
Anti-mouse CD11b APC-eFluor780 (clone: M1/70)	e-Bioscience	47-0112-80
Anti-mouse IL17 APC	e-Bioscience	17-7177-81
Anti-mouse IL4 APC	Tonbo	20-7041-U100
Anti-mouse IL5 APC	e-Bioscience	504306
Anti-mouse IL13 PE-Cy7	e-Bioscience	25-7133-82
Anti-mouse CD8α eFluor450	e-Bioscience	48-4321-82
Anti-mouse CD8α PerCP-eFluor710	e-Bioscience	46-0081-80

Anti-hu/mo CD45R(B220) AlexaFluor700 (clone:RA3-6B2)	e-Bioscience	56-0452-80
Anti-mouse STAT3 PerCP-Cy5.5 (Py705) (clone:4/P-STAT3 RUO)	BD	560114
Anti-mouse IL12(p40/70)PE (clone:C15.6)	BD	554480
Anti-mouse IDO1 AlexaFluor647 (clone:2E2/IDO1)	Biolegend	654004
PE Rat Anti-Mouse IL-2	BD	554428
CD45.1 APC-eFlour780	e-Bioscience	47-0453-80
Anti-Hu/Mo CD45R(B220) AlexaFluor700(clone:RA3-6B2)	e-Bioscience	56-0452-80
CFSE	Sigma	21888
Cell Proliferation Dye eFluor™ 670	e-Bioscience	65-0840-85
H/MpERK1/2(T202/Y204) PerCP-eFluor710 (clone:MILAN8R)	e-Bioscience	46-9109-42
Phospho-NF-κB p65 (Ser536) PE	CST	5733
Rabbit polyclonal to nuclear receptor corepressor	Abcam	ab24552
Rabbit polyclonal IgG NFkB p65(C-20)	Santa cruz	SC-372
Rabbit polyclonal IgG RelB (C-19)	Santa cruz	SC-226
Mouse monoclonal IgG PU.1 (Spi-1) (B-9)	Santa cruz	SC-390659
Mouse monoclonal RNA Pol-II (Rpb1) Ab	CST	2629
Rabbit monoclonal Histone H3 (D1H2)	CST	4499S
Rabbit monoclonal beta-Actin (D6A8)	CST	8457S
Rabbit monoclonal MyD88 (D80F5)	CST	4283S
Biotin anti-mouse IgG1	**Biolegend**	**406603**
Biotin anti-mouse IgG2b	Biolegend	406703
Biotin anti-mouse IgG2a	**Biolegend**	**407103**
Biotin anti-mouse IgG3	Biolegend	406803
HRP streptavidin	**Biolegend**	**405210**
Anti-mouse IgG-HRP	abcam	Ab97023
Donkey anti-mouse IgG-HRP	Santa cruz	SC-2314
Goat anti-rabbit IgG-HRP	**Santa cruz**	**SC-2004**
NF-kB p65	CST	8242S
RelB	**CST**	**10544s**
Histone H3(D1H2)	CST	4499S
Biological samples		
Heligmosomoids polygyrus	Nicola Harris (EPFL, Lausanne)	
Chemicals, Peptides, and Recombinant Proteins		

CpG ODN 1826	Invivogen	1826
Poly I:C (HMW)	Invivogen	TLRL-pic-5
LPS EB Ultrapure	Invivogen	TLRL-3 pelps
FLT3L serum	Transgenic mice	Baerenwaldt et al., 2016
Formaldehyde solution	Sigma	252549
Glycine	Sigma	50046
TMB ELISA substrate solution	e-Bioscience	00-4201-56
Gelatin	**Sigma**	**G1393**
CD8 T cell neutralizing antibody	Hybridoma	Clone H35
Critical Commercial Assays		
RNAeasy plus mini	Qiagen	74136
Superscript III	Invitrogen	180 80 044
Lightcycler 480 sybr green master	Roche	4887352001
Lightcycler 480 multiwell plate 96,white	Roche	04 729 692 001
Bio-plex pro mouse cytokine 23-plex	BIORAD	M60-009RDPD
BCA Protein assay kit	Thermo	PI-23227
Maxi WAVE Vertical Electrophoresis System	REPLIKA BIOTECK	MV-20WAVESYS
Calphos mammalian transfection kit	Takara	631312
NEBNEXT mRna library prep master mix set for illumina	NEB	E6100S
NEBNEXT chip-seq library prep master mix set for illumina	NEB	E6240S
NEBNEXT Poly(A) mrna Magnetic isolation module	NEB	E7490S
Foxp3/Transcription factor staining buffer set kit	ebiosciences	00-5523-00
CD4+ T cell isolation kit	Miltenyi biotec	130-104-454
Experimental Models: Cell Lines		
DC 1940 CD8a+ cell line	Fuertes Marraco et al., 2012	
CD11b cell line	This paper	
Experimental Models: Organisms/Strains		
NCoR1$^{fl/fl}$ mice	Johan Auwerx, EPFL, Lausanne	
Sequence-Based Reagents		
NCoR1 shRNA1 CCGGCCTCTAATACAGGCACTTCAACTCGAGTTGAA GTGCCTGTATTAGAGGTTTTTG	Sigma-Aldrich	Clone ID: NM_011308.2-7774s1c1
NCoR1 shRNA2 CCGGCGGCATAATCTTGACAACCTTCTCGAGAAGGT TGTCAAGATTATGCCGTTTTTG	Sigma-Aldrich	Clone ID: NM_011308.2-2269s1c1

NCoR1 shRNA3 CCGGCCAATAATTGAGGGTTCCATTCTCGAGAATGG AACCCTCAATTATTGGTTTTTG	Sigma-Aldrich	Clone ID: NM_011308.2-4381s1c1
NF-KB probe for EMSA G1 5'-GCTACAAGGGACTTTCCGCTGGGGACTTTCCAGGGA GG -3' G2 5' CCTCCCTGGAAAGTCCCCAGCGGAAAGTCCCTTGTA GC 3'	IDT	
Software and Algorithms		
Bowtie2	Langmead and salzberg 2012	http://bowtie-bio.sourceforge.net/bowtie2/manual.shtml
Tophat	Kim, pertea et al. 2013	https://ccb.jhu.edu/software/tophat/index.shtml
HOMER	Heinz, benner et al. 2010	http://homer.salk.edu/homer/
Cufflink	Trapnell, williams et al. 2010	http://cole-trapnell-lab.github.io/cufflinks/manual/
SeqMINER	Ye, krebs et al. 2011	http://bips.u-strasbg.fr/
ROSE	Whyte et al., 2013	https://bitbucket.org/young_computation/rose
ChIPseeker	Yu g, wang l and he q (2015)	http://bioconductor.org/packages/release/bioc/html/ChIPseeker.html

Gene expression primers		
Gene	**Sequence**	**source**
IL12b_F	GACTCCAGGGGACAGGCTA	IDT
IL12b_R	CCAGGAGATGGTTAGCTTCTGA	IDT
IL10_F	CAGAGCCACATGCTCCTAGA	IDT
IL10_R	TGTCCAGCTGGTCCTTTGTT	IDT
IL6_F	GCTACCAAACTGGATATAATCAGGA	IDT
IL6_R	CCAGGTAGCTATGGTACTCCAGAA	IDT
Actin_F	GGCTGTATTCCCCTCCATCG	IDT
Actin_R	CCAGTTGGTAACAATGCCATG	IDT
CD80_F	TCGTCTTTCACAAGTGTCTTCAG	IDT
CD80_R	TTGCCAGTAGATTCGGTCTTC	IDT
CD86_F	GAAGCCGAATCAGCCTAGC	IDT

CD86_R	CAGCGTTACTATCCCGCTCT	IDT
CD274/PDL1_F	CCATCCTGTTGTTCCTCATTG	IDT
CD274/PDL1_R	TCCACATCTAGCATTCTCACTTG	IDT
CCL2_F	CATCCACGTGTTGGCTCA	IDT
CCL2_R	GATCATCTTGCTGGTGAATGAGT	IDT
IL2_F	GCTGTTGATGGACCTACAGGA	GCC BIOTECH
IL2_R	TTCAATTCTGTGGCCTGCTT	GCC BIOTECH
IL27_F	GCAGGGAATTCACAGTCAGC	GCC BIOTECH
IL27_R	GGACATAGCCCTGAACCTCA	GCC BIOTECH
IDO1_F	GGGCTTTGCTCTACCACATC	IDT
IDO1_R	AAGGACCCAGGGGCTGTAT	IDT
IFNb1_F	CACAGCCCTCTCCATCAACTA	IDT
IFNb1_R	CATTTCCGAATGTTCGTCCT	IDT
NCOR1_F	TATGGACCGGGTAGACCGAG	IDT
NCOR1_R	CGGTGTTTTTGTTCCACAGGAG	IDT

ChIP primers		
Gene	**Sequence**	**Source**
Negative control 1 F	TGGCACAGTGAGCAAGTAGAA	GCC BIOTECH
Negative control 1 R	GAGGAGAGCTCGAGGGTAGG	GCC BIOTECH
Negative control 2 F	CCCTTCCAAATCTGTGTTACCT	GCC BIOTECH
Negative control 2 R	TCAACCACAGAACCAAGCAT	GCC BIOTECH
IL10 F	CTGACTTCTGCCTGGGGTAG	GCC BIOTECH
IL10 R	CCCTTATCCTCAAAGTCACGA	GCC BIOTECH
PDL1 or CD274 F	GTGATGGCCCATTTCTGAG	GCC BIOTECH
PDL1 or CD274 R	CAGCTGGCCAAACTAGCC	GCC BIOTECH
IL12a F	AGCACCTGTGTCTGAGTGGA	GCC BIOTECH
IL12a R	TTGTCTTCAAAGCCTCTGTCC	GCC BIOTECH
IRF8 F	CGTCTCTTGCTGTCAGGTCA	GCC BIOTECH
IRF8 R	CCCACTTGTGAGAGGTGAGAC	GCC BIOTECH
EBI3 F	AGTTCCCTCCTCTCCCTGTG	GCC BIOTECH
EBI3 R	CTTTCCTTCCGGCTGATG	GCC BIOTECH
PPARg F	TTGTGTTGATGTCACCAGAGG	GCC BIOTECH
PPARg R	AAACCAACTTGACAATTCTAGGAAC	GCC BIOTECH
CD40_F	GAGAAACTGGGTAGGGAACTCA	GCC BIOTECH
CD40_R	AAACGGGAAAGACCACAGC	GCC BIOTECH

CD83_F	AGGACTCATTTACTCCGCAGAT	GCC BIOTECH
CD83_R	AGGTTGTCAGGGCTACTAGTGTG	GCC BIOTECH
IL23a_F	AGGCCTAGGTCGGGACAC	IDT
IL23a_R	CCCCTTCTGCAGTCTTCTGT	IDT
EBI3 TSS_ F	TGTTTCTCTCAGTTCCCTCCTC	GCC BIOTECH
EBI3 TSS_ R	GTCACTGAGCAGCTTTCCTTC	GCC BIOTECH
IDO1 TSS_ F	CAAACCCCACAGCTGACAC	GCC BIOTECH
IDO1 TSS_ R	TGAAACTGTCCCAGGTGGA	GCC BIOTECH
IL10 TSS_ F	TCAAAAATTGCATGGTTTAGAAGA	GCC BIOTECH
IL10 TSS_ R	TTCCTGGCAAAGGTTTTTGT	GCC BIOTECH
IL12a TSS_ F	CGCAGCAAAGCAAGGTAAGT	GCC BIOTECH
IL12a TSS_ R	CCTCTAGATGCAGGGAGTTAGC	GCC BIOTECH
IL23a TSS_ F	GATCTGGCTGGCTCTGTGAT	GCC BIOTECH
IL23a TSS_ R	CCGCTTAGAAGTCGGACTACAG	GCC BIOTECH
IL27 TSS_ F	CCAAGGTCTCCTGTCACCTG	GCC BIOTECH
IL27 TSS_ R	GCAGCCCCCAGTATAAGACC	GCC BIOTECH
IRF8 TSS_ F	GACCTCATCTCCCTCCTCTCA	GCC BIOTECH
IRF8 TSS_ R	AGGCCTGAGGGTCAGAAACT	GCC BIOTECH
PPARg TSS_ F	CCGAGTGTGACGACAAGGT	GCC BIOTECH
PPARg TSS_ R	CACAGGCTCCTGTCAGAGTG	GCC BIOTECH
VDR TSS_ F	TCACCCAGAACCCCCTTC	GCC BIOTECH
VDR TSS_ R	CCAGGTGCTGAGCAGTCTCT	GCC BIOTECH
EBI3 IE_ F	ACGGTGCCCTACATGCTAAA	GCC BIOTECH
EBI3 IE_ R	AGGGAGGACAGACACTCACTG	GCC BIOTECH
IDO1 IE_ F	ACTAACCTCAGCCCCGGTA	GCC BIOTECH
IDO1 IE_ R	GGTTTCTCCACATCTCAATCG	GCC BIOTECH
IL10 IE_ F	CGGAAATGATCCAGTTTTACCT	GCC BIOTECH
IL10 IE_ R	CAAATGCTCCTTGATTTCTGG	GCC BIOTECH
IL12a IE_ F	ATCACAACCATCAGCAGATCA	GCC BIOTECH
IL12a IE_ R	AGGAAGGCTTACCTGCATCA	GCC BIOTECH
IL23a IE_ F	GCCCTATCTTCCAGATCCCTA	GCC BIOTECH
IL23a IE_ R	GAGCAACTTCACACCTCCCTA	GCC BIOTECH
IL27 IE_ F	TCAGGGAAACATTGGGAAGA	GCC BIOTECH
IL27 IE_ R	CACTGGCCCTCACTAACAGAA	GCC BIOTECH
IRF8 IE_ F	CACTCAGTGGTTTTTGGTTTCC	GCC BIOTECH
IRF8 IE_ R	TGAAATAGTGGGCTGTTTAGTCAT	GCC BIOTECH

PPARg IE_ F	CAAGCCCTTTACCACAGTTGA	GCC BIOTECH
PPARg IE_ R	CAGCTCTTGTGAATGGAATGTC	GCC BIOTECH
VDR IE_ F	GTGGGGTCGTAGGTCTTGTG	GCC BIOTECH
VDR IE_ R	TCTGAGGAGCAACAGCACAT	GCC BIOTECH